

# Coarsening process in one-dimensional surface growth models

Alessandro Torcini<sup>1,2,a</sup> and Paolo Politi<sup>2,b</sup>

<sup>1</sup> Dipartimento di Energetica “S. Stecco”, Università di Firenze, Via S. Marta 3, 50139 Firenze, Italy

<sup>2</sup> Istituto Nazionale per la Fisica della Materia, UdR Firenze, Via G. Sansone 1, 50019 Sesto Fiorentino, Italy

Received: date / Revised version: date

**Abstract.** Surface growth models may give rise to unstable growth with mound formation whose typical linear size  $L$  increases in time (coarsening process). In one dimension coarsening is generally driven by an attractive interaction between domain walls or kinks. This picture applies to growth models where the largest surface slope remains constant in time (corresponding to model B of dynamics): coarsening is known to be logarithmic in the absence of noise ( $L(t) \sim \ln t$ ) and to follow a power law ( $L(t) \sim t^{1/3}$ ) in the presence of it. If surface slope increases indefinitely, the deterministic equation looks like a modified Cahn-Hilliard equation whose late stages of coarsening we study here through a linear stability analysis of the stationary periodic configurations and through a direct numerical integration. Analytical and numerical results agree well in the conclusion that steepening of mounds makes deterministic coarsening *faster*: if  $\alpha$  is the exponent describing the steepening of the maximal slope  $M$  of mounds ( $M^\alpha \sim L$ ) we find that  $L(t) \sim t^n$ :  $n$  is equal to  $\frac{1}{4}$  for  $1 \leq \alpha \leq 2$  and it decreases from  $\frac{1}{4}$  to  $\frac{1}{5}$  for  $\alpha \geq 2$ , according to  $n = \alpha/(5\alpha - 2)$ . Contrastingly, the numerical solution of the corresponding stochastic equation clearly shows that in the presence of shot noise steepening of mounds makes coarsening *slower* than in model B:  $L(t) \sim t^{1/4}$ , irrespectively of  $\alpha$ . Finally, the presence of a symmetry breaking term is shown not to modify the coarsening law of model  $\alpha = 1$ , both in the absence and in the presence of noise.

**PACS.** 68. Surfaces and interfaces – 81.10.Aa Theory and models of film growth – 02.30.Jr Partial differential equations

## 1 Introduction

In real systems surface growth proceeds on two-dimensional (2d) substrates and therefore its modelization in one dimension (1d) is in general an oversimplification, mainly justified by the possibility to have a deeper understanding of the dynamical evolution of the system. In some cases the evolving 2d surface indeed maintains a 1d profile, for example when the relaxation of a grooved surface is studied [1]. This is no more true when the surface is kinetically roughened or if it undergoes a growth instability followed by a phase separation process: in all these cases noise makes the resulting morphology 2d even if the initial one is 1d.

The dynamical evolution of a vicinal surface, made up of atomic steps separated by terraces, can be an interesting application of 1d models, if all steps move in phase [2]: in this case the one-dimensional growth equation models the dynamics of the single step.

In this paper we are interested in a growing surface that undergoes a kinetic instability because diffusing adatoms must overcome a higher barrier to descend step edges (the so-called Ehrlich-Schwoebel (ES) barrier [3,4]). Even in the presence of stabilizing mechanisms, at sufficiently large scales the ES effect may dominate and the flat surface becomes unstable against small deformations. A structure with a well-defined wavelength emerges and its amplitude increases in time: this is the linear regime. Later on the nonlinearities come into play and the mound structure typically –but not unavoidably [2]– coarsens (late stage regime).

This simplified picture reminds spinodal decomposition and coarsening taking place during phase separation. The processes of surface growth instability and phase separation do have strong similarities, but important differences arise in two dimensions [5]. On the other hand, the parallel between unstable growth and phase separation is exact in one dimension [6].

Generally speaking qualitative differences exist between phase separation in one and two dimensions. We mention here two of them [7]: (i) In 2d coarsening is driven by the tension of domain walls while in 1d it is due to interaction between walls. (ii) Noise is generally irrelevant in 2d while

<sup>a</sup> e-mail: torcini@ino.it

<sup>b</sup> Corresponding author: e-mail: politi@fi.infn.it

it changes the coarsening law in 1d (except in the presence of long-range interactions).

The class of models we study in one dimension has some interest in both respects: firstly, since the slope is assumed to increase indefinitely it is not possible to speak of domain walls between different phases and it will be necessary to replace the interaction between domain walls with something different. Secondly, the interaction between these new ‘objects’ is long ranged and it may happen that noise is irrelevant for the coarsening law in 1d as well: this is indeed what occurs for some of the models here studied.

We aim at giving in the next Section a short introduction to the continuum equations that are encountered in one-dimensional models of conserved surface growth: more detailed analysis can be found in recent review papers [6, 8]. In Section 3 we recall a few theoretical approaches to one-dimensional coarsening and in Section 4 the linear stability analysis is applied to our class of deterministic  $\alpha$ -models; the results are confirmed by numerics. The problem of coarsening in the presence of noise is attacked directly by stochastic numerical integration in Section 5, while in Section 6 we examine the effect of a symmetry breaking term. The discussion of the results and our conclusions are presented in the final Section.

## 2 The models for unstable surface growth

In the Introduction we have already mentioned (i) the ES barriers as a source of the kinetic instability and (ii) possible stabilizing mechanisms. Point (i) simply expresses the well-known fact [9] that an asymmetry in the sticking coefficients of an adatom to a step produces a slope-dependent current  $j_{\text{ES}}(m)$ ;  $z(x, t)$  and  $m = \partial_x z$  are the local height and slope of the surface. For symmetry reasons  $j_{\text{ES}}$  is an odd function of  $m$  and therefore we expect that  $j_{\text{ES}} \simeq \nu m$  at small slopes, as confirmed by more rigorous analyses [6]. The asymmetry in the sticking coefficients is generally due to an additional energy barrier hindering the adatom to descend a step, which gives rise to an uphill current:  $j_{\text{ES}}$  is ‘parallel’ to  $m$  and the coefficient  $\nu$  is positive. This implies that it has a destabilizing character as easily revealed by the solution of the linear differential equation  $\partial_t z = -\partial_x j_{\text{ES}} = -\nu \partial_x^2 z(x, t)$ :  $z(x, t) = z_0 \cos(qx) e^{\omega_q t}$ , with  $\omega_q = \nu q^2$ . Different mechanisms may produce a slope-dependent current as well: short-range step-adatom interaction [3, 10], post-deposition transient mobility and downward funneling [11]. The first may be stabilizing or not, according to the sign of the step-adatom interaction while the other (non-thermal) mechanisms are typically stabilizing, i.e. they contribute with a negative term to  $j'_{\text{ES}}(0)$ .

All these possible different processes, once summed up, determine the form of the slope-dependent current  $j_{\text{ES}}$ . In the literature two main classes are considered, according to the presence (model 0) or the absence (model 1) of zeros at finite slope:

$$j_{\text{ES}} = \nu m(1 - m^2/m_0^2) \quad \text{model 0} \quad (1)$$

$$j_{\text{ES}} = \frac{\nu m}{1 + \ell_D^2 m^2} \quad \text{model 1} . \quad (2)$$

In a previous paper [12] we have generalized Eq. (2) to a class of models ( $\alpha$ -models) characterized by different asymptotic behaviors for  $m \rightarrow \infty$ :

$$j_{\text{ES}} = \frac{\nu m}{(1 + \ell_D^2 m^2)^\alpha} \quad \text{model } \alpha (\geq 1) . \quad (3)$$

The initial motivation for introducing such class of models had been the possibility to study the physically relevant model 1 in the limit  $\alpha \rightarrow 1^+$ . Anyway,  $\alpha$ -models revealed unexpected dynamical behaviour and therefore to have some interest by themselves.

We have briefly mentioned (see point (ii) at the beginning of this Section) possible stabilizing mechanisms. The simplest expression for a stabilizing current is the so-called Mullins term, that in its linearized form reads  $j_{\text{M}} = K \partial_x^2 m$ , and whose origin may be thermodynamic (relaxation through surface diffusion [13]) or kinetic (fluctuations in the nucleation process of new islands [14, 15]). A stabilizing current gives a negative contribution to  $\omega_q$ , but since it depends on higher order derivatives of the surface profile it is overcome by the unstable term at sufficiently large scales. As a matter of fact, starting from the equation  $\partial_t z = -\partial_x (j_{\text{ES}} + j_{\text{M}})$  it is easily found that  $\omega_q = \nu q^2 - K q^4$ , thus showing that the flat surface is linearly unstable against fluctuations of wavelength larger than  $\lambda_c = 2\pi \sqrt{K/\nu}$ .

Both currents  $j_{\text{ES}}$  and  $j_{\text{M}}$  change sign if  $x \rightarrow -x$  or  $z \rightarrow -z$ : the first symmetry can not be broken by the growth process but the second may and it is broken indeed. It has been shown [9, 14] that such symmetry breaking term (intrinsically nonlinear) has the form  $j_{\text{SB}} = \partial_x A(m^2)$ , where  $A \sim m^2$  at small slopes and  $A \sim -1/m^2$  at large ones. Its presence is strictly related to the breaking of the detailed balance principle [16] and therefore to the non-equilibrium character of the growth process.

It has been proven [17] that  $j_{\text{SB}}$  does not modify the coarsening law of model 0: for the moment  $j_{\text{SB}}$  is disregarded, but its effects on model 1 will be considered in Section 6.

We conclude by writing down explicitly the class of growth equations that are analyzed in the paper:

$$\partial_t z(x, t) = -\partial_x j(x, t) + \eta(x, t) \quad (4)$$

$$j(x, t) = \begin{cases} \partial_x^2 m + \frac{m}{(1+m^2)^\alpha} & \text{model } \alpha \\ \partial_x^2 m + m(1 - m^2) & \text{model 0} \end{cases} \quad (5)$$

$$\langle \eta(x, t) \rangle = 0 \quad \langle \eta(x, t) \eta(x', t') \rangle = \tilde{F}_0 \delta(x - x') \delta(t - t') \quad (6)$$

Eq. (4) is the evolution equation of the local height  $z(x, t)$  for a conserved growth process in the presence of the shot noise  $\eta(x, t)$ ; Eqs. (5) give the currents for the  $\alpha$ -models and model 0, once that  $x, t, z$  have been rescaled in order to get an adimensional equation; Eq. (6) gives the spectral properties of the noise, whose strength  $\tilde{F}_0 = F_0 a \ell^2 / \sqrt{\nu K}$  is the only parameter appearing in the problem:  $F_0$  is the intensity of the flux,  $a$  is the lattice constant,  $\ell$  is the diffusion length  $\ell_D$  for  $\alpha$ -models (Eqs. (2, 3)) or the inverse of the constant slope  $m_0$  for model 0 (Eq. (1)),  $\nu$  and  $K$  are the prefactors of  $j_{\text{ES}}$  and  $j_{\text{M}}$ , respectively.

### 3 Theoretical approaches to coarsening

In this Section we present two theoretical methods that have been used to study the coarsening process in model 0. The first uses the property that the current  $j_{\text{ES}}$  vanishes at a finite slope  $m_0$ . It can not be used for  $\alpha$ -models but for the sake of completeness and because it is quoted a few times in the paper we discuss it in Section 3.1. The second consists in a linear stability analysis of the stationary configurations. It is a very general method and it is discussed in Section 3.2. In the context of phase separation processes it was introduced by Langer [20] to study model 0 and its solution is proposed in Section 4.1. Its application to  $\alpha$ -models is carried out in Section 4.2.

#### 3.1 Kink dynamics

Model 0 and  $\alpha$ -models have the same linear behaviour, but it is apparent that they have strongly different nonlinear regimes: in the former case the slope increases up to the maximal value  $m_0 = \pm 1$  while in the latter case it may grow indefinitely.

For model 0, the surface profile corresponding to a constant value  $m_0 = 1$  (i.e. to a vicinal surface with unitary slope) is stable [18], but it can not be attained starting from a flat surface because the average slope must remain constant. Still, we can consider the stationary configuration  $m_+(x)$  ( $j(m_+(x)) \equiv 0$ ) corresponding to a limiting slope  $\pm m_0$  for  $x \rightarrow \mp\infty$ : that profile is called ‘mound’ in the  $z$ -space and ‘kink’ or ‘domain wall’ in the space of the order parameter  $m$ , where it has the form  $m_+(x) = \tanh(x/\sqrt{2})$ .

During the coarsening process of model 0 a generic surface profile is just an alternating sequence of kinks ( $m = m_+(x)$ ) and antikinks ( $m = m_-(x) = -m_+(x)$ ), whose average distance  $L(t)$  increases with time because of the annihilation process between pairs of neighbouring kink-antikink. In the absence of noise the dynamics of kinks is governed by their attractive interaction. An attraction that decays exponentially with the distance, since  $|m_{\pm}(x)| \simeq 1 - 2\exp(-\sqrt{2}|x|)$  for  $|x| \gg 1$ , and a so weak interaction determines a very slow coarsening:  $L(t) \sim \ln t$  [19, 20].

In the presence of noise the picture is different because of the induced fluctuations on the kink positions. If there were no constraint induced by the conservation of the order parameter, kinks would simply carry out a random walk and therefore would travel a distance  $L$  in a typical time  $L^2$ , giving a coarsening exponent  $n = 1/2$  ( $L(t) \sim \sqrt{t}$ ). In a growth process, where a conservation law does exist, kink motions are not independent and the coarsening slows down:  $n = 1/3$ . This exponent is more easily understood in a spin picture [21], where the conservation of the order parameter (the magnetization) implies that the system evolves through spin-exchange processes (Kawasaki dynamics).

If we turn now to  $\alpha$ -models we recognize that the kink picture is not applicable because the unstable current  $j_{\text{ES}}$  vanishes for infinite slope only. Nonetheless we will show

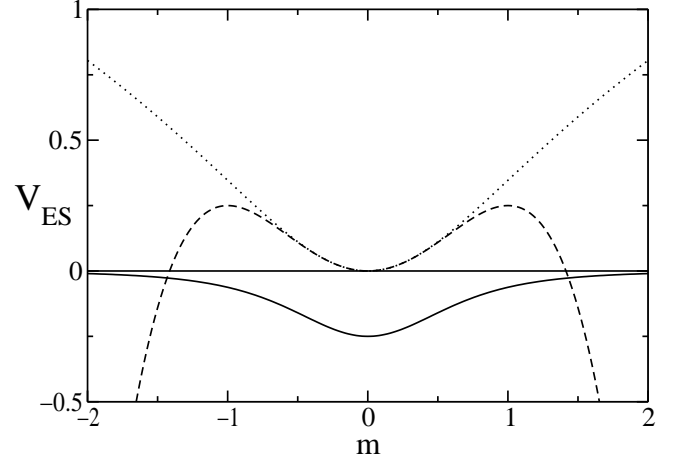


**Fig. 1.** Profiles of the different potentials  $V_{\text{ES}}$ . From top to bottom: Model 1 (dotted line), Eq. (9); Model 0 (dashed line), Eq. (8); Model  $\alpha = 3$  (full line), Eq. (10).

in the following that kinks may be replaced by different objects playing a similar role: this is indeed true only for  $\alpha$  strictly larger than one and that is the reason why model 1 can not be treated directly, but just in the limit  $\alpha \rightarrow 1$ . It can be solved numerically anyhow, and this confirms the validity of taking the limit.

#### 3.2 Linear stability analysis of stationary configurations

We introduce now the linear stability analysis of the stationary configurations; so, we need to determine all the time-independent solutions of the evolution equation. The condition  $\partial_t z(x, t) \equiv 0$  implies that the current must be a constant:  $j \equiv c$ . The net current  $c$  is related to the average slope of the surface: we are interested in a high symmetry one and therefore  $c = 0$ .

The equation  $j = 0$  is easily recognized as the Newton’s equation for a particle of unitary mass, where the slope  $m$  plays the role of the particle position and  $x$  the role of time:

$$\partial_x^2 m(x) + j_{\text{ES}}(m) = 0. \quad (7)$$

The fictitious particle feels the force  $-j_{\text{ES}}(m)$ , i.e. it moves in the potential  $V_{\text{ES}}(m) = \int^m ds j_{\text{ES}}(s)$ . Different models give qualitatively different potentials (see Fig. 1):

$$V_{\text{ES}}(m) = m^2/2 - m^2/4 \quad \text{model 0} \quad (8)$$

$$V_{\text{ES}}(m) = (1/2) \ln(1 + m^2) \quad \text{model 1} \quad (9)$$

$$V_{\text{ES}}(m) = -(1 + m^2)^{1-\alpha}/[2(\alpha - 1)] \quad \text{model } \alpha > 1 \quad (10)$$

Stationary configurations therefore correspond to the periodic oscillations of the particle around the minimum of  $V_{\text{ES}}$  in  $m = 0$ . We label the stationary configurations through their period  $2L$ :  $m_{2L}(x)$ . What about the limit  $L \rightarrow \infty$ ? For model 0 it corresponds to the kink-solution:  $m_{\infty}(x) = m_+(x) \rightarrow \pm 1$  when  $x \rightarrow \pm\infty$ . For model 1, the energy of the particle diverges when the period  $L$  increases

and the limiting configuration  $m_\infty(x)$  does *not* exist. Contrastingly, it does exist for  $\alpha > 1$  and it corresponds to the well defined problem of a particle of zero energy moving in the potential (10): it leaves from  $m = -\infty$  and arrives after an infinite time at  $m = +\infty$ .

We start by considering small deviations  $\psi$  from the periodic profile:  $m(x, t) = m_{2L}(x) + \psi(x, t)$ . Since  $j_{\text{ES}}(m_{2L} + \psi) = j_{\text{ES}}(m_{2L}) + j'_{\text{ES}}(m_{2L})\psi + \mathcal{O}(\psi^2)$ , we obtain that the linearized evolution equation for  $\psi(x, t)$  is

$$\partial_t \psi = \partial_x^2 [-\psi''(x, t) - j'_{\text{ES}}(m_{2L}(x))\psi] \quad (11)$$

and therefore the time dependence of  $\psi$  is:  $\psi(x, t) = \phi(x) \cdot \exp(-\epsilon t)$ , giving exponentially decreasing ( $\epsilon > 0$ ) or increasing ( $\epsilon < 0$ ) solutions. The former case corresponds to a stable fluctuation and the latter to a unstable one.

Replacing the expression of  $\psi$  in terms of  $\phi$  into Eq. (11), we find that the stability is determined by the spectrum of the following operator:

$$(-\partial_x^2) [-\phi''(x) + U_L(x)\phi] \equiv D_x \hat{H} \phi(x) = \epsilon \phi, \quad (12)$$

where  $D_x \equiv -\partial_x^2$  and  $\hat{H} \equiv -\partial_x^2 + U_L(x)$  is a single-particle Schroedinger operator corresponding to the periodic potential  $U_L(x) \equiv -j'_{\text{ES}}(m_{2L}(x))$ , of period  $L$ :

$$\begin{aligned} U_L(x + L) &= -j'_{\text{ES}}(m_{2L}(x + L)) \\ &= -j'_{\text{ES}}(-m_{2L}(x)) = U_L(x). \end{aligned} \quad (13)$$

In one dimension coarsening is due to the unstable character of the periodic stationary configurations, i.e. to the existence of negative eigenvalues in the energy spectrum [22]. Because of the periodic character of the operator  $D_x \hat{H}$ , eigenvalues are grouped in separated energy bands.

Our evolution equation for  $m(x, t)$  is  $\partial_t m = D_x j$  where the current  $j$  (see Eq. (5)) can be derived from a pseudo free energy  $\mathcal{F}$ :

$$j = -\frac{\delta \mathcal{F}}{\delta m} \quad \mathcal{F} = \int dx [\frac{1}{2}(\partial_x m)^2 - V_{\text{ES}}(m)] \quad (14)$$

For model 0 the potential  $-V_{\text{ES}}(m)$  has the standard double well shape and  $m(x, t)$  evolves accordingly to the Cahn-Hilliard equation; in the presence of conserved noise we obtain the so-called model B of dynamics [23]. If the operator  $D_x$  is replaced by the identity operator, the order parameter is no more conserved and its evolution equation is  $\partial_t m = j$ , which is equivalent for model 0 to the time dependent Ginzburg Landau equation, or –in the presence of nonconserved noise– to model A of dynamics [23].

It is for this reason that studying the spectrum of the operator  $\hat{H}$  is not only necessary but useful as well, since it allows to discuss the coarsening properties of the non-conserved models. In order to avoid any confusion we use the notations  $\tilde{\epsilon}, \tilde{\phi}$  for the spectrum of the operator  $D_x \hat{H}$  ( $D_x = -\partial_x^2$ ) and  $\epsilon, \phi$  for the Hamiltonian operator  $\hat{H}$ .

Let us start with few general statements on the lowest part of the spectrum. Translational invariance implies that

$\epsilon = 0$  is always an eigenvalue of the operator  $\hat{H}$  (and therefore  $\tilde{\epsilon} = 0$  is an eigenvalue of  $D_x \hat{H}$  as well) and it corresponds to the eigenfunction  $\phi(x) (= \tilde{\phi}(x)) = m'_{2L}(x)$ . To prove it let us use the definition of  $m_{2L}(x)$  as solution of the differential equation (7) and take its derivative:

$$m'''_{2L}(x) + j'_{\text{ES}}(m_{2L})m'_{2L}(x) = 0. \quad (15)$$

Since  $U_L(x) = -j'_{\text{ES}}(m_{2L}(x))$  we just have

$$-\partial_x^2(m'_{2L}(x)) + U_L(x)(m'_{2L}(x)) \equiv \hat{H}m'_{2L}(x) = 0. \quad (16)$$

Therefore the operators  $\hat{H}$  and  $D_x \hat{H}$  have a zero energy eigenvalue and the corresponding eigenfunction  $m'_{2L}(x)$  has period  $\lambda = 2L$  (i.e. it corresponds to the wavevector  $q = \pi/L$  in the Bloch representation).

We can now recognize the importance of the limit  $m_\infty(x)$ . If  $m_\infty(x)$  exists the periodic potential  $U_L(x)$  in the limit  $L \rightarrow \infty$  becomes a single well potential  $U_\infty(x)$ . In this limit  $m_{2L}(x)$  is a monotonic function  $m_+(x)$  (the kink solution, for model 0). Therefore  $\tilde{\phi}_1(x) = \phi_1(x) \equiv m'_+(x)$  has no node and it must represent the ground state for the single well problem. For finite  $L$  we have a periodic potential and the energy level  $\epsilon_1 = \tilde{\epsilon}_1 = 0$  opens to give rise to the lowest band of the spectrum. The ground state  $\epsilon_{\text{GS}}(L)$  of the operator  $\hat{H}$  corresponds to  $q = 0$  and it therefore must have a negative energy, implying that  $\hat{H}$  has negative eigenvalues. The relation  $\tilde{\epsilon}_{\text{GS}} = \tilde{\epsilon}(q = 0)$  is no more true for the conserved model, but Langer [20] has shown that negative eigenvalues  $\epsilon$  of  $\hat{H}$  may be put in correspondance to negative eigenvalues  $\tilde{\epsilon}$  of  $D_x \hat{H}$  (see Section 4.1).

Since an unstable mode increases exponentially with the factor  $\exp(|\epsilon|t)$ , the knowledge of the  $L$  dependence of the ground state energy allows to find the deterministic coarsening law  $L(t)$  via the relations  $|\epsilon_{\text{GS}}(L)| \sim 1/t$  (non-conserved model) and  $|\tilde{\epsilon}_{\text{GS}}(L)| \sim 1/t$  (conserved model).

## 4 Deterministic coarsening: results

In Fig. 2 we plot the single well potentials  $U_\infty(x)$  for model 0 (dashed line) and for model  $\alpha = 3$  (full line), the latter being representative of all the class of  $\alpha$ -models. Since we have explained that  $\epsilon_1 = 0$  is the ground state energy for the single well it is apparent that completely different behaviours are expected in the two cases.

For model 0 (see Section 4.1),  $U_\infty(x)$  tends at large  $x$  to a strictly positive constant value (equal to 2); therefore the wavefunction  $\phi_1(x)$  decays exponentially at large distances and energy shifts due to the tunneling between wells at finite distance  $L$  are expected to be exponentially small. This property is the counterpart of the exponentially vanishing interaction between kinks, discussed in Section 3.1.

For  $\alpha$ -models (see Section 4.2),  $U_\infty(|x| = \infty) = 0 = \epsilon_1$  and the considerations developed for model 0 no more apply. We will see how coarsening laws are affected by this.

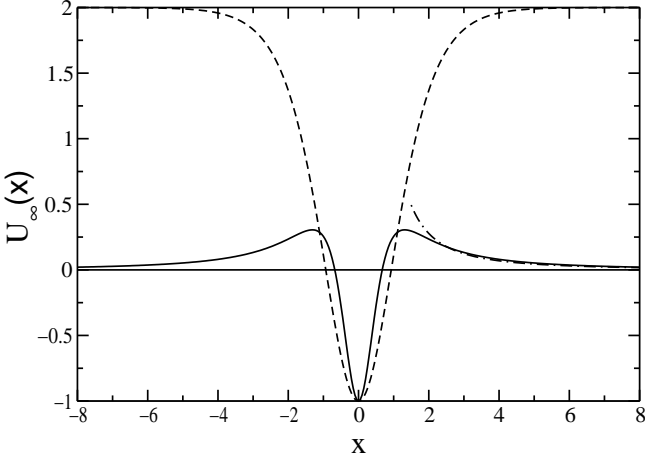


**Fig. 2.** The single well potential  $U_\infty(x)$  for model 0 (dashed line) and for model  $\alpha = 3$  (full line). At large  $x$  the former goes to a positive constant value (equal to 2) while the latter goes to zero, with the asymptotic behaviour  $U_\infty(x) = a/x^2$  with  $a = 10/9$  (dashed-dotted line, see formula (25)).

#### 4.1 Model 0

For model 0 the kink-solution is  $m_\infty(x) = \tanh(x/\sqrt{2})$ , the single well potential is (see the dashed line in Fig. 2)

$$U_\infty(x) = -1 + 3m_\infty^2(x) = -1 + 3 \tanh^2(x/\sqrt{2}) \quad (17)$$

and the corresponding ground state wavefunction is  $\phi_1(x) = m'_\infty(x) = \frac{1}{\sqrt{2}} \sec^2(\frac{x}{\sqrt{2}})$ .

For finite  $L$ ,  $U_L(x)$  is a collection of wells centred at points  $x = 0, \pm L, \pm 2L, \dots$ . It is interesting to compare  $U_L(x)$  with the periodic potential  $U_L^*(x)$  obtained as a superposition of the single well potentials  $U_\infty(x - nL)$ :

$$U_L^*(x) = U_\infty(x) + \sum_{n \neq 0} [U_\infty(x - nL) - U_\infty(\infty)] \quad (18)$$

For model 0,  $U_\infty(\infty) = 2$  and the summation can indeed be limited to the two terms  $n = \pm 1$  because the quantity in square brackets is exponentially small. In Fig. 3a we compare  $U_L(x)$  (circles) with  $U_L^*(x)$  (full line) and they perfectly agree: this proves that for model 0 the periodic potential  $U_L(x)$  is actually given by the superposition of the single well potentials  $U_\infty(x - nL)$ .

Langer performed a tight-binding-approximation to determine the lowest band of the energy spectrum which arises from the ground state level  $\epsilon_1 = 0$  of the single well. The result [20] is

$$\epsilon(q) \simeq -(1 + \cos qL) \exp(-2L), \quad (19)$$

confirming that  $\epsilon(q = \pi/L) = 0$ , that  $\epsilon_{\text{GS}} = \epsilon(q = 0)$  and that  $\epsilon_{\text{GS}}$  decays exponentially with the distance  $L$  between wells. The relation  $|\epsilon_{\text{GS}}| \sim 1/t$  [24] implies that coarsening is logarithmically slow:  $L(t) \sim \ln t$ . This result is valid for the *conserved* model as well. Langer proved it through the following variational condition [20]:

$$\tilde{\epsilon}_{\text{GS}} \leq \frac{\epsilon_{\text{GS}}}{(\phi_1, \phi_1)} \quad (20)$$

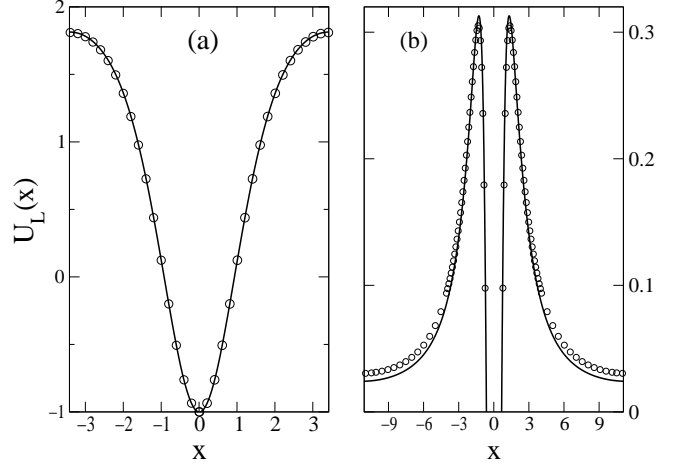


**Fig. 3.** The true periodic potential  $U_L(x)$  (empty circles) is compared with the potential  $U_L^*(x)$  (full line), obtained as a superposition of the single well potentials  $U_\infty(x - nL)$  (see Eq. (18)). We make this comparison for model 0 (a), where  $L \simeq 6.8$ , and for model  $\alpha = 3$  (b), where  $L \simeq 22.8$ . In both cases we display one period only.  $U_L(x)$  is obtained numerically and  $U_L^*(x)$  is obtained analytically. The superposition principle works well in (a) even for small  $L$ , while the exact potential for model 3 (see b) is *not* reproduced by the sum of single well potentials. In order to make more evident the difference between the two potentials, in (b) we focus the plot on the region of positive  $U_L(x)$ . We remind that  $U_L(0) = -1$  whatever is the model.

where

$$(\bar{\phi}_1, \phi_1) = \int dx \bar{\phi}_1^*(x) \phi_1(x) \quad (21)$$

is the scalar product between the ground state function  $\phi_1(x)$  of the Hamiltonian operator and  $\bar{\phi}_1$  is defined by the relation  $D_x \bar{\phi}_1 = \phi_1$ .

Because of the conservation law, the lowest energy band for the operator  $D_x \hat{H}$  reads [20]:

$$\epsilon(q) \simeq -\sin^2 qL \cdot \frac{\exp(-2L)}{L}. \quad (22)$$

The factor  $L$  at denominator is irrelevant and the coarsening law  $L(t) \sim \ln t$  is still valid. Eq. (22) also confirms that  $\tilde{\epsilon}(q = \pi/L) = 0$  and that  $\tilde{\epsilon}(q = 0)$  is no more the ground state.

#### 4.2 $\alpha$ -models

The solution of model 0 by Langer has a lot of interest because it gives approximate expressions for the lowest energy band, both for the nonconserved (19) and conserved (22) models. The basis of his treatment was the tight-binding-approximation, where  $U_L(x)$  is replaced by  $U_L^*(x)$  and  $\Delta U(x) \equiv U_L^*(x) - U_\infty(x)$  is taken as a small perturbation of the single well potential  $U_\infty(x)$ .

In a previous Letter [12] we have performed a much simpler treatment of the energy shift, for  $\alpha$ -models: we

replaced the periodic potential  $U_L(x)$  with a double well  $U_2(x)$  and secondly we took the double well potential as obtained by joining rather than superposing the two single well potentials  $U_\infty(x)$  and  $U_\infty(x-L)$  [25]. In spite of these approximations our analytical results for the coarsening exponent  $n(\alpha)$  agreed well with its determination through numerical integration of the growth equations [12] (see the results for the conserved model reported in Fig. 9). In the following we put forth the general lines of this theoretical approach, and we add a direct numerical confirmation (see Fig. 4).

The single well potential  $U_\infty(x)$  for the  $\alpha$ -models is seen in Fig. 2 to decay to zero at large  $x$  from positive values. From the relation  $U_\infty(x) = -j'_{\text{ES}}(m_\infty(x))$  it is simple to derive that for  $m \gg 1$ :

$$U_\infty(x) \sim \frac{(2\alpha - 1)}{m_\infty^{2\alpha}(x)}. \quad (23)$$

The integration of Newton's equation (7) for an energy of the particle equal to zero therefore gives the asymptotic result ( $x \gg 1$ ):

$$m_\infty^\alpha(x) \sim \frac{\alpha}{\sqrt{\alpha-1}} x, \quad (24)$$

which implies

$$U_\infty(x) \sim \frac{(2\alpha - 1)(\alpha - 1)}{\alpha^2} \frac{1}{x^2} \equiv \frac{a}{x^2}. \quad (25)$$

Thus the single well potential decays as the inverse of a square law *whatever* is  $\alpha$ , but with a prefactor  $a$  that increases between  $a = 0$  for  $\alpha = 1$  and  $a = 2$ , for  $\alpha = \infty$ . For  $\alpha = 3$ ,  $a = \frac{10}{9}$  and the corresponding function  $\frac{a}{x^2}$  is reported in Fig. 2 as the dashed-dotted line, showing the comparison between the asymptotic expansion (25) and the exact expression [26].

The solution  $\phi_1(x)$  of the Schroedinger equation for the single well (let us remind that the ground state has zero energy) therefore decays at large  $x$  as a power law [12]:  $\phi_1(x) \sim |x|^{-\beta}$ , with  $\beta = (1 - \alpha^{-1})$ . So, the ground state wavefunction is a bound state for  $\beta > \frac{1}{2}$  i.e.  $\alpha > 2$  only.

In Ref. [12] we used the Landau and Lifshitz approach [27] for the problem of the double well and we extended it to take into account the possibility that the ground state wavefunction for the single well is not a bound state, that happens for  $1 < \alpha \leq 2$ . The main point is that even if  $\phi_1(x)$  is not a bound state, the ground state  $\phi_2(x)$  of the double well *is* bound, because its energy  $\epsilon_2$  is now strictly negative and so lower than the asymptotic value  $U_2(\infty) = 0$ ,  $U_2(x)$  being the double well potential.

According to the above approach we found [12] that

$$|\epsilon_{\text{GS}}(L)| \simeq L^{-\gamma} \quad \gamma = \begin{cases} 2 & \alpha < 2 \\ (3 - \frac{2}{\alpha}) & \alpha > 2 \end{cases}. \quad (26)$$

Once that  $\gamma$  is known, the coarsening exponent  $n$  is just given by  $n = 1/\gamma$ . In Table 1 we summarize the results found in Ref. [12] for the nonconserved and conserved models. For  $\alpha = 2$  there are logarithmic corrections:  $L \sim (t/\ln t)^n$ .

**Table 1.** The deterministic coarsening exponent  $n$ , for the nonconserved ( $D_x \equiv 1$ ) and the conserved ( $D_x \equiv -\partial_x^2$ ) models. For  $\alpha = 2$  there are logarithmic corrections (see [12]).

	$1 < \alpha < 2$	$\alpha > 2$
nonconserved	$\frac{1}{2}$	$\frac{\alpha}{3\alpha-2}$
conserved	$\frac{1}{4}$	$\frac{\alpha}{5\alpha-2}$

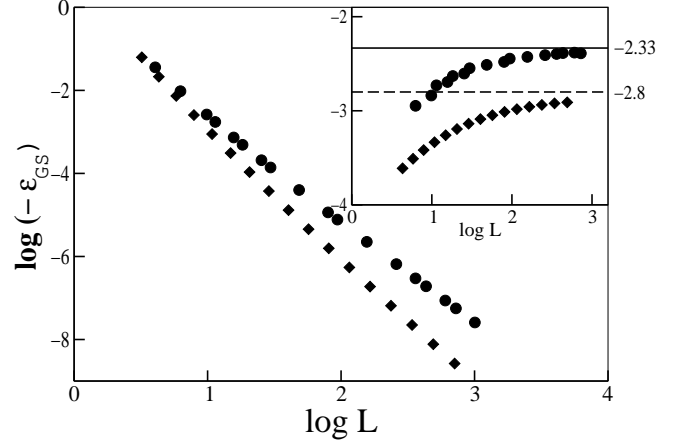


**Fig. 4.** Nonconserved models: on a log-log scale (main) we report the absolute value of the ground state energy  $\epsilon_{\text{GS}}(L)$  for the periodic potential  $U_L(x)$ . Circles refer to model 3 and diamonds to model 10. In the inset we report the local derivatives  $d[\log(-\epsilon_{\text{GS}})]/d[\log(L)]$  and the asymptotic values of  $\gamma$  that are calculated analytically (see Eq. (26)).

The reason why it has not been possible to treat the periodic potential  $U_L(x)$  in a more rigorous way is given in Fig. 3b, where it is clearly shown that the superposition principle does *not* work for  $\alpha$ -models: accordingly the potential  $U_L(x)$  can not be approximated as the sum of single-well potentials and therefore the application of the tight-binding-approximation is not straightforward because we do not know the explicit expression of the perturbation  $\Delta U(x) \equiv U_L(x) - U_\infty(x)$ . The disagreement between  $U_L(x)$  and  $U_L^*(x)$  might appear at first sight to be negligible, but if we neglect it (and we have tried to do it) we obtain wrong results.

However, it is possible to check *in a direct way* the accuracy of our theory: we solve numerically the quantum mechanical problem to determine the ground state energy  $\epsilon_{\text{GS}}(L)$  of the full periodic potential  $U_L(x)$  (see Fig. 4 and footnote [28]). The numerical results for the exponent  $\gamma$  agree fairly well, at large  $L$ , with the theoretical predictions  $\gamma(3) = 2.3$  and  $\gamma(10) = 2.8$ . This confirms that our theoretical approach to calculate  $\epsilon_{\text{GS}}(L)$  is indeed correct.

### 4.3 Numerical analysis

Let us now discuss our numerical results for the deterministic  $\alpha$ -models. We have numerically integrated the equa-

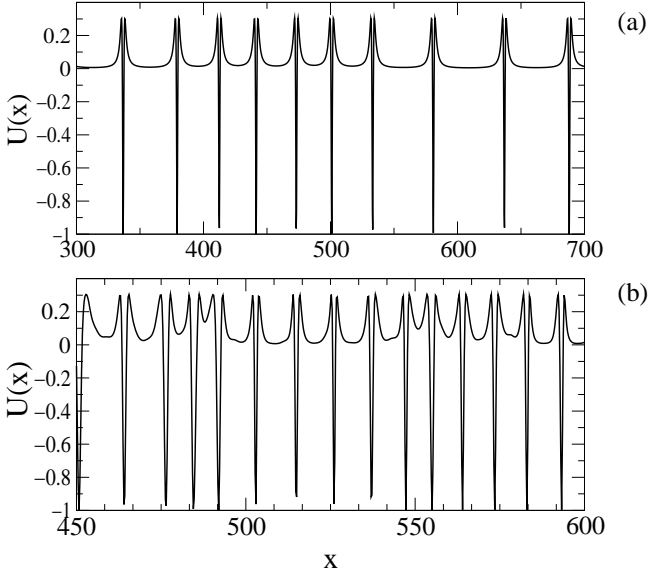


**Fig. 5.** Model  $\alpha = 3$ , late stages of coarsening. We have taken the profile  $m(x, t) = z'(x, t)$  as obtained via numerical integration of  $z(x, t)$  and we have evaluated  $U(x) = -j'(m)$ . We display only a piece of the total spatial domain. (a)  $U(x)$  in the absence of noise. (b)  $U(x)$  in the presence of shot noise (single realization).

tion of motion (4) for the field  $z(x, t)$ , starting from an initial profile  $z(x, 0) = r_x$ , where  $r_x$  is a random variable with a flat distribution in the interval  $[-0.1, 0.1]$ .

Typically, we have followed the dynamical evolution for a total time  $t_{\text{MAX}} \sim 400,000 - 1,600,000$ , for a chain length  $L_c = 1024$ , with a spatial resolution  $\delta x = 0.25$  and an integration time step  $\tau = 0.05$ . A few tests have been also performed with a smaller time step  $\tau = 0.025$  and with longer chains ( $L_c = 2048 - 4096$ ), obtaining consistent results. The adopted integration scheme is a time-splitting pseudo-spectral code: more details are reported in App. A.1.

Once  $z(x, t)$  has been integrated numerically we can easily determine, through the relation  $U(x) = -j'_{\text{ES}}(z'(x, t))$ , the potential  $U(x)$  that enters in the analytical solution of the problem (see the previous section). It is therefore reassuring (see Fig. 5a) that it looks indeed as a regular sequence of the single well potentials depicted in Fig. 2 as a full line, because it confirms that the surface profile keeps close to a stationary configuration.

The next step is to evaluate the characteristic length  $L(t)$ , corresponding to the average distance between wells. We define a characteristic wavevector  $p_c(t)$  via the relation:

$$p_c(t) = \frac{\sum_p' p S(p, t)}{\sum_p' S(p, t)}. \quad (27)$$

where  $S(p, t) = |\tilde{z}(p, t)|^2$  is the power spectrum associated to the field  $z$  at time  $t$  ( $\tilde{z}$  being its spatial Fourier transform) and the sum is restricted to the wavevectors  $p$  for which  $S(p) \geq \delta \cdot S_M$ ,  $S_M$  being the maximum value of

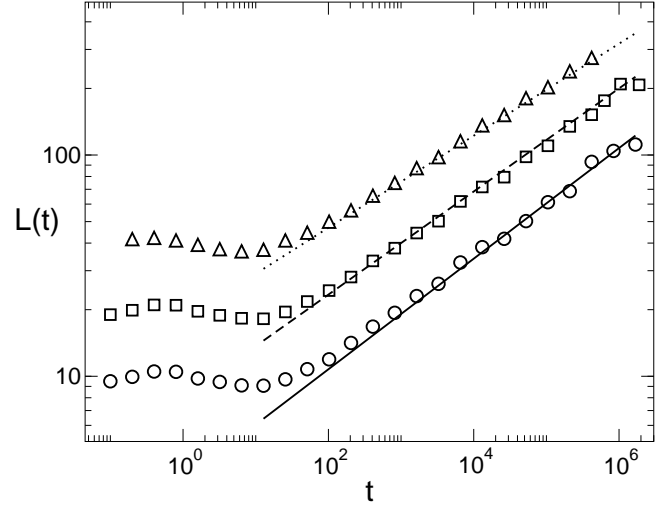


**Fig. 6.** Deterministic coarsening:  $L$  vs  $t$  in log-log scale for  $\alpha = 1.5$  ( $\circ$ ),  $\alpha = 3$  ( $\square$ ) and  $\alpha = 10$  ( $\triangle$ ). For presentation purpose the data for  $\alpha = 3$  and 10 are shifted by a constant. The lines indicate the best fit to the data for  $t > 10,000$  and the slopes are equal to 0.250 (—), 0.233 (---) and 0.208 ( $\cdots$ ), in agreement with the theoretical prediction (see Table 1).

the spectrum and  $\delta$  some threshold (typical values are  $\delta \sim 0.1 - 0.2$ ). The characteristic length is then evaluated as  $L(t) = 2\pi/p_c(t)$  and the coarsening exponent  $n(\alpha)$  has been obtained by considering the scaling behaviour of  $L(t) \sim t^n$  in a time interval  $10,000 < t < 400,000 - 1,600,000$ .

As an independent check we have also determined  $L$  from the normalized spatial correlation function of the surface profile

$$C(r, t) = \frac{\langle z(x+r, t)z(x, t) \rangle - \langle z(x, t) \rangle^2}{\langle z(x, t)^2 \rangle - \langle z(x, t) \rangle^2}, \quad (28)$$

where the spatial average  $\langle \cdot \rangle$  is performed along the chain. Defining  $L$  through the relation

$$C(L, t) = C(0, t)/2 \quad (29)$$

our results are in agreement with the previous ones obtained from the power spectrum, in all the cases considered.

The numerical estimated length  $L(t)$  is reported in Fig. 6 for  $\alpha = 1.5, 3, 10$ . The coarsening exponents are  $n(1.5) = 0.250 \pm 0.003$ ,  $n(3) = 0.233 \pm 0.005$  and  $n(10) = 0.208 \pm 0.002$ . These results are consistent with the theoretical estimates for  $n(\alpha)$ , as shown by the comprehensive Fig. 9. Their critical discussion is deferred to the final section.

## 5 Coarsening with conservative noise

The stochastic equation (4) has been integrated up to a time  $t_{\text{MAX}} \sim 800,000$  with  $L_c = 1024$ . The results for  $L(t)$  and  $C(r, t)$  have been obtained by averaging over a

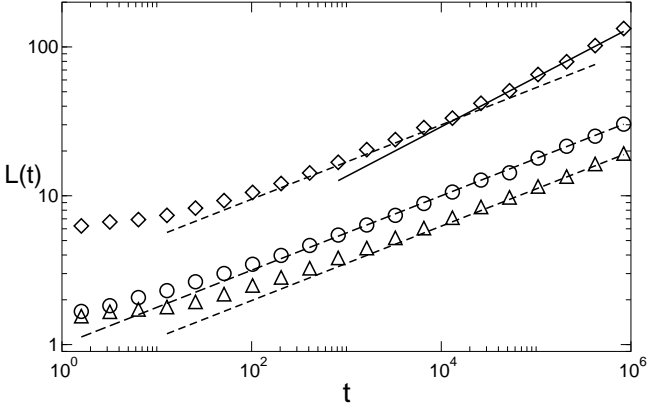


**Fig. 7.** Coarsening in the presence of shot noise:  $L$  vs  $t$  in log-log scale for model 0 ( $\diamond$ ) and for  $\alpha = 1$  ( $\triangle$ ) and  $\alpha = 10$  ( $\circ$ ). Dashed lines have slope  $1/4$  and full line has slope  $1/3$ .

certain number of different initial conditions  $N_c$  with different noise realizations (typically  $N_c = 10$ ). The integration scheme employed in the noisy case is different from the one adopted for the deterministic integration and it is described in detail in App. A.2. We have used a noise strength corresponding to a value of  $\tilde{F}_0$  (see Eq. (6)) equal to 0.05. This is a physically reasonable value because for a large ES effect [6],  $\tilde{F}_0 \approx \frac{a}{\ell_D}$  and  $\ell_D$  is typically of the order of a few dozens of lattice constants.

In Fig. 5b we show the potential  $U(x)$  in the presence of shot noise as obtained through the numerical integration of  $z(x, t)$ : a sequence of single wells is clearly visible, but it is less clean than in Fig. 5a. We want to remark that plotting  $U(x) = -j'(z'(x, t))$  gives a more explicit piece of information than plotting the surface profile  $z(x, t)$  or its derivative  $m(x, t)$ , because for  $\alpha$ -models  $U_\infty(x)$  has a more defined and recognizable shape than  $m_\infty(x)$ .

For the noisy case we have defined  $L$  only in term of the average correlation function  $\overline{C(r, t)}$ , where the bar means that average is now performed at each time not only along the chain (see definition (28)) but also over different noise realizations. A sufficiently good scaling is obtained in the time interval  $40,000 < t < 800,000$  for all the considered values of  $\alpha$  ( $= 1, 2, 10$ ).

As a benchmark to verify the validity of our integration scheme as well as of our procedure to estimate  $n(\alpha)$  we have firstly analyzed model 0. It is known [19,20] that the coarsening exponent is  $n = 1/3$ , and indeed a good agreement between our numerical data and the theoretical prediction is found for  $t > 40,000$ , as shown in Fig. 7. For two values of  $\alpha$  as different as  $\alpha = 1$  and  $\alpha = 10$  we find the same value  $n = 1/4$ . We are therefore led to conclude that in the presence of shot noise the coarsening exponent is independent of  $\alpha$  and equal to  $1/4$ . Fig. 7 also suggests the possible existence for model 0 of an intermediate regime (with  $L \sim 5 - 20$ ) where an effective exponent  $n = \frac{1}{4}$  is found.

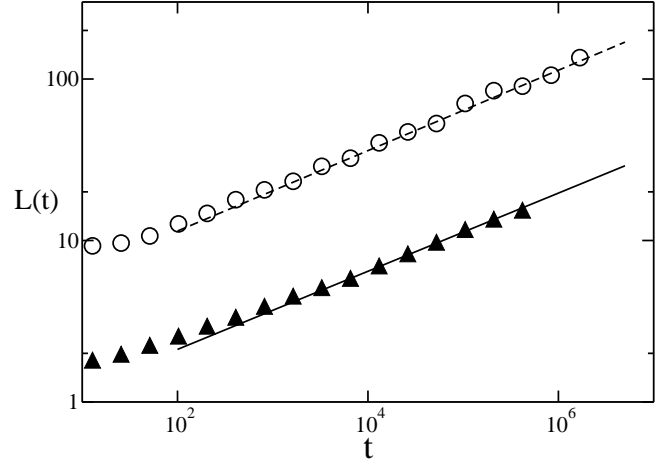


**Fig. 8.** Coarsening for the asymmetric model (Eq. (31) with  $\lambda^* = 1$ ), in the absence (empty circles) and in the presence (full triangles) of shot noise. Fits have been done for  $t > 10^4$  and give  $n = 0.25$  without noise (dashed line) and  $n = 0.24$  with noise (full line). Circles have been shifted by a constant.

## 6 Effects of a symmetry breaking term

In Ref. [17] one of us studied the effect of symmetry breaking on model 0. Since in that model the slope keeps finite with a maximal value equal to one, the detailed expression of the function  $A(m^2)$  ( $j_{\text{SB}} = \partial_x A$ ) is not so relevant. It was therefore chosen the simplest form, the one valid at small slopes:  $A(m^2) = \lambda^* m^2$ .

Contrastingly, for  $\alpha$ -models the slope can diverge so that the exact expression of  $j_{\text{SB}}$  should be employed [14]:

$$j_{\text{SB}} = -\lambda^* \partial_x \left( \frac{1}{1 + m^2} \right). \quad (30)$$

We have confined ourselves to study the physically relevant case  $\alpha = 1$ : we have therefore integrated the following differential equation:

$$\partial_t z = -\partial_x \left[ \partial_x^2 m + \frac{m}{1 + m^2} - \lambda^* \partial_x \left( \frac{1}{1 + m^2} \right) \right] + \eta \quad (31)$$

for values of  $\lambda^*$  varying between 0.1 and 1.

Our results (see Fig. 8) suggest that  $j_{\text{SB}}$  is *irrelevant* for the coarsening law, both for  $\eta \equiv 0$  (deterministic case) and for  $\eta \neq 0$  (noisy case).

## 7 Discussion and conclusions

In Fig. 9 we have summarized our numerical and theoretical results for the coarsening exponent  $n$  ( $L \sim t^n$ ). In the absence of noise our theory (full line) predicts that  $n = \frac{1}{4}$  for  $1 < \alpha \leq 2$  and for larger values of  $\alpha$  it decreases down to  $\frac{1}{5}$  ( $n = 1/(5 - \frac{2}{\alpha})$ ). Numerical results (full circles) agree well with the full line.



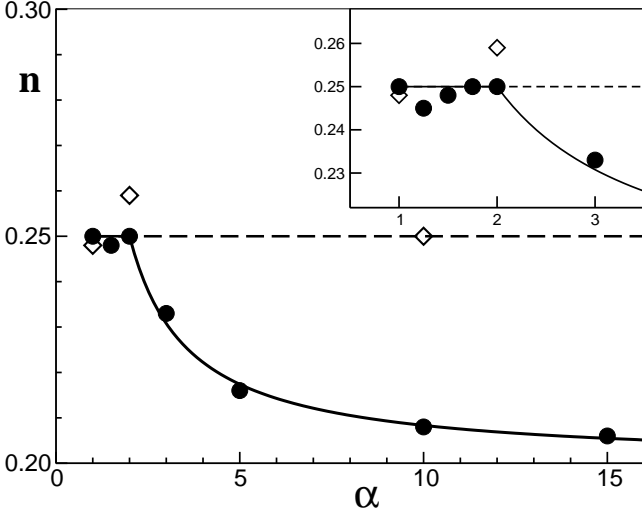


**Fig. 9.** The coarsening exponent  $n$  as a function of  $\alpha$ , for the deterministic models (full circles) and for the stochastic models (open diamonds). In the inset we enlarge the region of small  $\alpha$ . Full line is the theoretical result in the absence of noise (Table 1) and the dashed line is our ansatz  $n = 1/4$  for the noisy case.

We know of only one analytical paper treating our class of models (Ref. [29]): therein the author uses scaling arguments to conclude that *in the absence* of noise  $n = 1/4$  irrespectively of  $\alpha$  and for any dimension  $d$  of the substrate. A drastically simplified version of the scaling arguments runs as follows. If  $Z, L$  and  $M = Z/L$  are respectively the typical height, width and slope of mounds at time  $t$ , the evolution equation for  $z(x, t)$  implies  $Z/t \sim j/L$ . The current  $j$  is made up of the Mullins term, of order  $M/L^2$  plus the ES current, whose asymptotic expression for large slope is  $1/M^{2\alpha-1}$ . They vanish in the limit  $t \rightarrow \infty$  and must be of the same order in  $1/t$ , which entails the relation  $M^\alpha \sim L$ . If their sum  $j$  is supposed to be of the same order as well, the relation  $Z/t \sim M/L^3$  implies  $L(t) \sim t^{1/4}$ , i.e.  $n = 1/4$  for any  $\alpha$ .

A problem of this argument is that the two terms appearing in  $j$  are of the same order but their sum is smaller (i.e. of higher order in  $1/t$ ) because of a compensation effect. This is a necessary condition otherwise stationary configurations would not play any role in the coarsening process; on the contrary we have proved that the values  $n(\alpha)$  for the deterministic models can be determined via linear stability analysis of such stationary solutions.

In order to have a direct numerical check of our statement we have evaluated the following quantities as a function of time:  $\langle |\partial_x j_M| \rangle$ ,  $\langle |\partial_x j_{ES}| \rangle$  and  $\langle |\partial_x (j_M + j_{ES})| \rangle$ , where  $\langle \dots \rangle$  means, as before, the spatial average. For all the considered values of  $\alpha$  ( $\alpha = 1, 3, 10$ ), the result is the same: the ratio  $\langle |\partial_x j_M| \rangle / \langle |\partial_x j_{ES}| \rangle$  is equal to one, up to higher order terms, and  $\langle |\partial_x (j_M + j_{ES})| \rangle / \langle |\partial_x j_M| \rangle$  goes to zero.

Our numerical results tell even more than that: in fact scaling arguments would suggest that  $n$  is strictly smaller than  $1/4$  if  $j$  is smaller than  $j_M$  and  $j_{ES}$ , but for  $\alpha \leq 2$  we do find  $n = 1/4$  even if  $|j|/|j_M| \simeq |j|/|j_{ES}| \rightarrow 0$ .

Model  $\alpha = 1$  had been previously studied numerically at short times in Ref. [30] and authors found a value  $n \approx 0.22$ , independent of the noise strength.

Let us now discuss the results in the presence of noise. Fig. 9 presents with diamonds the numerical results for the stochastic integration of Eq. (4). Our data refer to  $\alpha = 1, 2, 10$  and provide a reasonably convincing evidence that in the presence of noise the coarsening exponent remains constant,  $n = 1/4$  (dashed line). The somewhat larger value for  $\alpha = 2$  may be due to unknown logarithmic corrections.

Authors in Refs. [31, 32] use qualitative arguments to describe coarsening assisted by noise: they use a ‘single mound’ model and set the coarsening time through the requirement that shot noise induces a height fluctuation of the same order of the mound height. In one dimension they find  $n = 1/(3 + \frac{2}{\alpha})$ , where  $\alpha$  is defined phenomenologically through the asymptotic relation  $M \sim L^{1/\alpha}$  between the typical (or the maximal) slope  $M$  and the width  $L$  of mounds.

Such prediction for  $n(\alpha)$  seems to agree with the result  $n = 1/3$  for model 0 because in that model the slope is constant and therefore it can effectively be equivalent to the model  $\alpha = \infty$ . Actually, if we take the limit  $\alpha = \infty$  in our class of  $\alpha$ -models (see Eq. (5)) it is straightforward to conclude that the current  $j_{ES}$  just vanishes for  $\alpha = \infty$  and we obtain the linear equation:

$$\partial_t z(x, t) = -\partial_x^4 z(x, t) + \eta(x, t). \quad (32)$$

The basic question is whether our class of  $\alpha$ -models tends –in some sense– or not to Eq. (32) with increasing  $\alpha$ . In the absence of noise the answer is surely negative: we have explained in several places how the existence of stationary solutions of increasing period is crucial for the deterministic coarsening, but Eq. (32) does not have such solutions.

If noise is present ( $\eta \neq 0$ ), Eq. (32) describes a process of kinetic roughening: the growing surface is characterised by a correlation length  $\tilde{\xi}(t) \sim t^{1/\tilde{z}}$  whose time dependence follows a power law with an exponent simply given by the inverse of the so-called dynamical critical exponent  $\tilde{z}$ . In  $d = 1$  it is well known [4] that for the quartic linear equation (32),  $\tilde{z} = 4$  and  $\tilde{\xi}(t) \sim t^{1/4}$ . It is reasonable to guess that the stochastic  $\alpha$ -model does converge to Eq. (32) for  $\alpha \rightarrow \infty$  and –in the same limit–  $n(\alpha) \rightarrow \frac{1}{\tilde{z}} = \frac{1}{4}$ .

What is the meaning of a constant value  $n = 1/4$  for any  $\alpha$ ? It is simple: in the presence of noise the detailed form of the current  $j_{ES}$  is irrelevant provided that the slope  $m$  diverges.

We can now summarize our main results. Without noise,  $n = 1/4$  for  $\alpha \leq 2$  and  $n = 1/(5 - \frac{2}{\alpha})$  for  $\alpha > 2$ . This result has been obtained analytically and it has been confirmed by extensive numerical calculations. It can not be deduced by simple scaling arguments. In the presence of noise our numerical data for  $\alpha = 1, 2, 10$  suggest that  $n = 1/4$  irrespectively of  $\alpha$ . This guess agrees with the well known result  $\tilde{\xi}(t) \sim t^{1/4}$ , valid for the linear model  $\alpha = \infty$ . So, steepening of mounds makes coarsening faster without noise and slower with noise.

We believe that the surface profile can not be described as a sequence of mounds with a spatially constant slope  $M$  that increases in time: this may be the reason of the failure of the qualitative arguments for determining  $n$  and that assume this picture.

We have also considered the possible existence of a symmetry breaking term  $j_{SB}$  in the current: for model 1, as already proved for model 0 [17], it is irrelevant.

We conclude the paper by mentioning a modification of model 0, extensively studied by Bray and Rutenberg [33], whose coarsening properties have some similarities with our  $\alpha$ -models: it consists in the addition of a long-range attraction between kinks. If such interaction decays with the distance as a power law ( $1/L^s$ , with  $s > 1$ ) the deterministic coarsening exponent is found to be  $n = 1/(1+s)$ . In the presence of conservative noise, this appears to be relevant for  $s > 2$  and in that case  $n = \frac{1}{3}$ . Some analogies therefore exist with our class of  $\alpha$ -models, because in both cases the coarsening exponent is a continuously varying function of a parameter ( $\alpha$  or  $s$ ), in both cases noise may change ( $\alpha, s > 2$ ) or not ( $1 < \alpha, s \leq 2$ ) the exponent, in both cases the stochastic coarsening exponent is constant if noise is relevant.

We warmly thank Claudio Castellano for a detailed and critical reading of the manuscript. We also acknowledge useful discussions with Andrea Crisanti and David Mukamel.

## A Details on the integration algorithms

Let us rewrite in an explicit way the evolution equation (4) for the field  $z(x, t)$ :

$$\partial_t z(x, t) = -\partial_x^4 z - \partial_x \left[ \frac{\partial_x z}{(1 + (\partial_x z)^2)^\alpha} \right] + \eta(x, t) \quad , \quad (33)$$

where  $\eta(x, t)$  indicates additive  $\delta$ -correlated spatio-temporal gaussian noise, i.e.

$$\langle \eta(x, t) \rangle = 0 \quad (34)$$

$$\langle \eta(x, t) \eta(0, 0) \rangle = \tilde{F}_0 \delta(x) \delta(t) \quad . \quad (35)$$

### A.1 Deterministic equation

Let us first neglect the noise term: in order to perform the numerical integration of (33) we consider a discrete spatial grid of resolution  $\delta x$  and a discrete time evolution with time step  $\tau$ . The discretized field is written as  $z(i, n)$ , where the integer indices  $i$  and  $n$  are the spatial and temporal discrete variables, respectively. Periodic boundary conditions have been considered for the field:  $z(i, n) = z(i + I, n)$ , where  $I$  is the number of sites of the grid ( $L_c = I\delta x$ ). The algorithm adopted to integrate (33) is a time-splitting pseudo-spectral code [34]. In particular, by following [35] Eq.(33) has been rewritten as

$$\partial_t z(x, t) = (\mathcal{L} + \mathcal{N})z(x, t) \quad (36)$$

where  $\mathcal{L}$  and  $\mathcal{N}$  are two operators defined in the following way:  $\mathcal{L}z = -\partial_x^4 z$  and  $\mathcal{N}z = -\partial_x \left[ \frac{\partial_x z}{(1 + (\partial_x z)^2)^\alpha} \right]$ . As usual for time splitting algorithms, the linear evolution, ruled by the operator  $\mathcal{L}$ , is treated independently from the nonlinear one (associated to the operator  $\mathcal{N}$ ). A complete evolution over an integration time step  $\tau$  therefore corresponds to the two successive integration steps:

$$z^*(x, t + \tau) = \exp[\mathcal{L}\tau]z(x, t) \quad (37)$$

and

$$z(x, t + \tau) = \exp[\mathcal{N}\tau]z^*(x, t + \tau) \quad (38)$$

where  $z^*(x, t)$  is a dummy field.

Let us firstly consider the linear part,

$$\partial_t z(x, t) = \mathcal{L}z(x, t) \quad . \quad (39)$$

Eq.(39) can be easily solved in the Fourier space and the equation of motion for the spatial Fourier transform of the field  $\tilde{z}(p, t)$  is

$$\partial_t \tilde{z}(p, t) = -p^4 \tilde{z} \quad . \quad (40)$$

The time evolution for  $\tilde{z}$  is simply given by

$$\tilde{z}^*(p, t + \tau) = \exp[-p^4 \tau] \tilde{z}(p, t) \quad . \quad (41)$$

Therefore, in order to integrate Eq.(39), the field should be Fourier transformed in space ( $\mathcal{F}$ ), then multiplied by the propagator reported in Eq.(41) and the outcome of such operation should be finally inverse-Fourier transformed ( $\mathcal{F}^{-1}$ ):

$$z^*(x, t + \tau) = \mathcal{F}^{-1} \exp[-p^4 \tau] \mathcal{F}z(x, t) \quad . \quad (42)$$

The integration of the nonlinear part has been performed by employing a second-order Adam-Basforth scheme

$$z(x, t + \tau) = z^*(x, t + \tau) + \frac{\tau}{2} [3G(z(x, t)) - G(z(x, t - \tau))] \quad , \quad (43)$$

where  $G(z(x, t)) = \left\{ -\partial_x \left[ \frac{\partial_x z}{(1 + (\partial_x z)^2)^\alpha} \right] \right\}$ . In order to obtain a better precision, the spatial derivatives appearing in  $G(z(x, t))$  have been evaluated in the Fourier space.

### A.2 Noisy equation

Let us now consider the noisy problem: in this case the algorithm outlined here above does not guarantee a sufficient precision. Therefore, we have developed a more accurate integration scheme [36] that consists as a first step in rewriting the equation of motion (33) in the Fourier space

$$\partial_t \tilde{z}(p, t) = -p^4 \tilde{z}(p, t) + G_p(z, t) + \tilde{\eta}(p, t) \quad , \quad (44)$$

where  $G_p(z, t)$  and  $\tilde{\eta}(p, t)$  are the Fourier transforms of the nonlinear part and of the noise term appearing in Eq. (33). The amplitudes  $\tilde{\eta}(p, t)$  of the noise components

in the Fourier space are still gaussian  $\delta$ -correlated stochastic variables with zero average and with a variance  $\mathcal{V}_p = \mathcal{F}_0/I$  independent of  $p$  (white noise). The formal exact solution of (44) is

$$\tilde{z}(p, t + \tau) = e^{-p^4 \tau} \left[ \tilde{z}(p, t) + \int_t^{t+\tau} dt' e^{p^4(t'-t)} (G_p(z, t') + \tilde{\eta}(p, t')) \right]. \quad (45)$$

The problem is now to evaluate the two terms appearing in the integral. The first term has been evaluated adopting a second order Adam-Bashfort scheme. i.e.

$$\int_t^{t+\tau} dt' e^{p^4(t'-t)} G_p(z, t') = \frac{\tau}{2} \left[ 3G_p(z, t) - e^{-p^4 \tau} G_p(z, t - \tau) \right] + \mathcal{O}(\tau^3). \quad (46)$$

The treatment of the second term is more delicate, since it is a stochastic integral: we have chosen to evaluate it accordingly to the Ito's prescription [37]:

$$\int_t^{t+\tau} dt' e^{p^4(t'-t)} \tilde{\eta}(p, t') = [W_p(t + \tau) - W_p(t)] = \Delta W_p(t). \quad (47)$$

Here  $W_p(t)$  and  $\Delta W_p(t)$  represent two Wiener processes: in particular we have  $\langle \Delta W_p \rangle = 0$  and  $\langle (\Delta W_p)^2 \rangle = \tau \mathcal{V}_p$ . The complete solution of (44) can be written as

$$\tilde{z}(p, t + \tau) = e^{-p^4 \tau} \tilde{z}(p, t) + \frac{3\tau}{2} e^{-p^4 \tau} G_p(z, t) - \frac{\tau}{2} e^{-2p^4 \tau} G_p(z, t - \tau) + e^{-p^4 \tau} \Delta W_p(t). \quad (48)$$

In order to obtain the solution in the real space it is sufficient to inverse-Fourier transform  $\tilde{z}(p, t + \tau)$ .

Due to the spatial and temporal discreteness of the integration scheme, the spatio-temporal noise term  $\eta(x, t)$  should be rewritten as  $\gamma_i^n$ , where  $\gamma$  is a random gaussian variable of zero average and variance

$$\mathcal{V} = \frac{\tau \tilde{F}_0}{\delta x}, \quad (49)$$

with

$$\langle \gamma_i^n \gamma_0^0 \rangle = \mathcal{V} \delta_{i,0} \delta_{n,0}. \quad (50)$$

The spatio-temporal discrete gaussian noise, with zero average and standard deviation  $\sqrt{\frac{\tau \tilde{F}_0}{\delta x}}$  has been numerically generated by employing a Box-Muller algorithm [34].

## References

1. A. Chame, S. Rousset, H.P. Bonzel and J. Villain, Bulg. Chem. Commun. **29**, 398 (1996/97) and references therein.
2. O. Pierre-Louis, C. Misbah, Y. Saito, J. Krug, P. Politi, Phys. Rev. Lett. **80**, 4221 (1998).
3. K. Kyuno, G. Ehrlich, Surf. Sci. **383**, L766 (1997) and references therein.

4. A. Pimpinelli, J. Villain, *Physics of crystal growth* (Cambridge, Cambridge University Press, 1998).
5. M. Siegert, Physica A **239**, 420 (1997); M. Siegert, Phys. Rev. Lett. **81**, 5481 (1998); D. Moldovan, L. Golubovic, Phys. Rev. E **61**, 6190 (2000).
6. P. Politi, G. Grenet, A. Marty, A. Ponchet, J. Villain, Phys. Rep. **324**, 271 (2000).
7. A.J. Bray, Adv. Phys. **43**, 357 (1994).
8. J. Krug, Adv. Phys. **46**, 139 (1997).
9. J. Villain, J. de Physique I **1**, 19 (1991).
10. J.G. Amar, F. Family, Phys. Rev. Lett. **77**, 4584 (1996).
11. J.W. Evans, Phys. Rev. B **43**, 3897 (1991).
12. P. Politi, A. Torcini, J. Phys. A: Math. Gen. **33**, L77 (2000).
13. W.W. Mullins, J. Appl. Phys. **28**, 333 (1957).
14. P. Politi, J. Villain, Phys. Rev B **54**, 5114 (1996).
15. P. Politi, J. Villain, in *Surface Diffusion: atomistic and collective processes*, edited by M.C. Tringides (Plenum Press, New York, 1997) p. 177.
16. Z. Rácz, M. Siegert, D. Liu, M. Plischke, Phys. Rev. A **43**, 5275 (1991).
17. P. Politi, Phys. Rev. E **58**, 281 (1998).
18. A linear stability analysis of a 1d vicinal surface of constant slope  $m^*$  shows that step-flow is stable if  $j'_{ES}(m^*) < 0$ .
19. K. Kawasaki, T. Ohta, Physica A **116**, 573 (1982); T. Kawakatsu, T. Munakata, Prog. Theor. Phys. **74**, 11 (1985).
20. J.S. Langer, Ann. Phys. **65**, 53 (1971).
21. S.J. Cornell, K. Kaski, R.B. Stinchcombe, Phys. Rev. B **44**, 12263 (1991).
22. Strictly speaking negative eigenvalues are a necessary but not a sufficient condition to ensure coarsening.
23. P.C. Hohenberg, B.I. Halperin, Rev. Mod. Phys. **49**, 435 (1977).
24. The exact relation, as derived by Langer [20] is  $t^{-1} = \sum_q |\epsilon(q, L)|$  where the sum is restricted to the negative (and therefore unstable) modes. However, the  $L$  dependence of  $\epsilon$  can be pulled out the summation and it is therefore sufficient to consider the ground state energy.
25. Joining means that  $U_2(x) = U_\infty(x)$  for  $x \leq \frac{L}{2}$  and  $U_2(x) = U_\infty(x - L)$  for  $x \geq \frac{L}{2}$ . This kind of juxtaposition is used by Landau and Lifshitz [27] in their treatment of the double well problem and for model 0 it gives the correct results.
26. The Newton's equation for the model  $\alpha = 3$  can be easily integrated if the particle has zero energy and therefore an explicit expression for  $U_\infty(x)$  is available. We do not report it here, but we write explicitly the first correction to the leading order in the large  $x$  expansion:  $U_\infty(x) \simeq \frac{10}{9x^2} + (\frac{16}{9})^{1/3} \frac{1}{x^{8/3}}$ . At  $x = 10$  the first correction is of order of one quarter of the leading term.
27. L.D. Landau, E.M. Lifshitz, *Quantum mechanics: non-relativistic theory* (Oxford, Pergamon Press, 1977). Section 50, Problem 3.
28. In order to find the ground state energy we have imposed periodic boundary conditions and searched for the zero node wavefunction. Precision real\*16 has been necessary in order to achieve a sufficient precision at large  $L$ .
29. L. Golubović, Phys. Rev. Lett. **78**, 90 (1997).
30. A.W. Hunt, C. Orme, Williams, B. G. Orr, L.M. Sander, Europhys. Lett. **27**, 611 (1994); L.M. Sander, private communication.
31. J. Krug, in *Nonequilibrium statistical mechanics in one dimension*, edited by V. Privman (Cambridge University Press, Cambridge, 1997), p. 305.

- 32. Lei-Han Tang, P. Šmilauer, D.D. Vvedensky, Eur. Phys. J. B **2**, 409 (1998).
- 33. A.J. Bray, A.D. Rutenberg, Phys. Rev. E **49**, R27 (1994); A.D. Rutenberg, A.J. Bray, Phys. Rev. E **50**, 1900 (1994).
- 34. W.H. Press, *et al.*, *Numerical Recipes* (Cambridge University Press, Cambridge, 1988).
- 35. D. Goldman and L. Sirovich, Quart. Appl. Math. **53** 315 (1995); A. Torcini, H. Frauenkron, and P. Grassberger, Phys. Rev. E **55** (1997) 5073; M. Nitti, A. Torcini, and S. Ruffo, Int. J. Mod. Physics C **10** (1999) 1039.
- 36. A. Crisanti, private communication
- 37. C.W. Gardiner, *Handbook of Stochastic Methods for Physics, Chemistry and the Natural Sciences* (Springer-Verlag, 1983, Berlin)